RESEARCH

UDOT CONNECTING COMMUNITIES

Utah Department of Transportation - Research Division
4501 South 2700 West, Box 148410 - Salt Lake City, Utah 84114-8410

Report No. UT-10.04

REPAIR OF PRESTRESSED CONCRETE GIRDER ENDS AND GIRDER COLLISION REPAIR

Prepared For:

Utah Department of Transportation Research Division

Submitted By:

University of Utah
Department of Civil & Environmental Engineering

Authored By:

Chris P. Pantelides, Ph.D.
Lawrence D. Reaveley, Ph.D.
Clayton A. Burningham

January 2010

DISCLAIMER

The authors alone are responsible for the preparation and accuracy of the information, data, analysis, discussions, recommendations, and conclusions presented herein. The contents do not necessarily reflect the views, opinions, endorsements, or policies of the Utah Department of Transportation and the US Department of Transportation. The Utah Department of Transportation makes no representation or warranty of any kind, and assumes no liability therefore.

THIS PAGE INTENTIONALLY LEFT BLANK

REPORT TECHNICAL DOCUMENTATION PAGE

1. Report No.	2. Government Accession No.	3. Recipient's Catalog No.
UT-10.04		

4. Title and Subtitle	5. Report Date
REPAIR OF PRESTRESSED CONCRETE GIRDER ENDS AND GIRDER COLLISION REPAIR	JANUARY, 2010
	6. Performing Organization Code
7. Author	8. Performing Organization Report No.
Chris P. Pantelides, Ph.D. Lawrence D. Reaveley, Ph.D. Clayton A. Burningham	
9. Performing Organization Name and Address	10. Work Unit No.
University of Utah Department of Civil and Environmental Engineering 122 S. Central Campus Dr. Ste. #204 Salt Lake City, Utah 84112	Job: 5H062H7H
	11. Contract or Grant No.
	089113
12. Sponsoring Agency Name and Address	13. Type of Report & Period Covered
Utah Department of Transportation 4501 South 2700 West Salt Lake City, Utah 84114-8410	FINAL Nov. 2007-Dec. 2009
	14. Sponsoring Agency Code
	PIC No. UT07.805

15. Supplementary Notes

Prepared in cooperation with the Utah Department of Transportation

16. Abstract

Many bridges in the Unites States are ageing such that they are in need of repair or strengthening. Fiber reinforced polymer composites are an increasingly popular material that can be used for bridge girder retrofit/repair. The purpose of this research, therefore, is to develop methods and design guidelines for repair and retrofit of bridge girders suffering (1) shear strength deficiencies related to end cracking and (2) flexural strength deficiencies related to vehicular collision. Scaled test specimens were fabricated and subjected to cyclic loading in order to instigate damage similar to that caused by end cracking and vehicular collision. Subsequently, the damaged specimens were repaired with external post-tensioned carbon fiber rods and re-tested to failure. This report presents the data from the tests and design guidelines for the use of external post-tensioned carbon fiber rods for repair applications.

17. Key Words	18. Distribution Statement	23. Registrant's Seal
Girder repair, girder retrofit, shear repair, vehicle impact repair, prestressed concrete, FRP	UDOT Research Division 4501 South 2700 West-box 148410 Salt Lake City, Utah 84114	

19. Security Classification	20. Security Classification	21. No. of Pages	22. Price
Unclassified	Unclassified	58	

THIS PAGE INTENTIONALLY LEFT BLANK

ACKNOWLEDGEMENTS

The authors wish to thank the Utah Department of Transportation for funding this project. Additionally, the authors would like to thank Brandon Besser, Mark Bryant, Megan Crump, Jack Furbush, Mike Gibbons, Ruifen Liu, Brett Raddon, Eric Smith, Max Wood, and Arthur Yeomans for their assistance in fabricating and testing the specimens. The authors acknowledge Hanson Eagle Precast for their donation of prestressed concrete girders used in the research and Geneva Rock Products, Inc. for their donation of concrete used in the casting of the reinforced concrete specimens.

THIS PAGE INTENTIONALLY LEFT BLANK

TABLE OF CONTENTS

DISCLAIMER I

ACKNOWLEDGEMENTS V

TABLE OF CONTENTS VII

EXECUTIVE SUMMARY 1

1.0 INTRODUCTION 3

1.1 Background Information 3

1.2 Project Scope 3

1.3 Report Outline 5

2.0 RESEARCH METHODS 7

2.1 Overview 7

2.2 Specimen Fabrication 7

2.3 Experimental Design 9

2.4 Testing Methods and Loading Protocol 9

2.4.1 Initial Damage Loading 10

2.4.2 FRP Repair 12

2.4.3 Loading To Failure 12

3.0 DATA COLLECTION 15

3.1 Overview 15

3.2 Data collection Methods 15

3.3 Instrumentation Locations 15

4.0 DATA ANALYSIS 17

4.1 Overview 17

4.2 Material Properties 17

4.3 RC Specimen Data Analysis 17

4.4 PC Specimen Data Analysis 21

4.5 Design Equations 24

4.5.1 RC Specimen Design Equations 24

4.5.2 PC Specimen Design Equations 26

APPENDIX A: B12 (CONTROL) CAPACITY CALCULATIONS 31

APPENDIX B: B8 (REPAIRED) CAPACITY CALCULATIONS 37

APPENDIX C: P1 (REPAIRED) AND P2 (CONTROL) CAPACITY CALCULATIONS 39

REFERENCES 43

ACRONYMS 45

LIST OF FIGURES

Figure 1 – Girder end damage - 200 East Bridge at I-80 4
Figure 2 – Girder damage caused by vehicular impact - I-80 bridge in Wanship, UT 4
Figure 3 – Reinforcement layout for specimen B8 8
Figure 4 – Reinforcement layout for specimens P1 and P2 8
Figure 5 – Test setup 10
Figure 6 – Loading protocol for specimen B8 11
Figure 7 – Damaged outer steel tendon in specimen P1 11
Figure 8 – End view of two level stressing system 13
Figure 9 – Side view of two level stressing system 13
Figure 10 – Specimen B12 LVDT locations 16
Figure 11 – Specimen P1 LVDT locations 16
Figure 12 – Force vs. midspan deflection plot for specimen B12 (control) 18
Figure 13 – Force vs. midspan deflection plot for specimen B8 (repaired) 19
Figure 14 – Specimen B12 (control) after concrete failure 19
Figure 15 – Specimen B8 (repaired) after CFRP rod rupture and concrete failure 20
Figure 16 – Force vs. midspan deflection plot for reinforced concrete specimens 20
Figure 17 – Specimen P1 (repaired) after CFRP rod rupture 21
Figure 18 – Specimen P2 (control) after concrete compressive failure 22
Figure 19 – Force vs. midspan deflection plot for prestressed concrete specimens 23
Figure 20 – Elongation in damaged outer steel tendon in specimen P1 (repaired) 24
Figure 21 – B12 (control) strut-and-tie model 25
Figure 22 – B8 (repaired) strut-and-tie model 25

THIS PAGE INTENTIONALLY LEFT BLANK

LIST OF TABLES

Table 1 – Summary of specimen geometric and reinforcement properties 9
Table 2 – RC specimen peak loads and factors of safety 26
Table 3 – PC specimen peak loads and factors of safety 27

THIS PAGE INTENTIONALLY LEFT BLANK

EXECUTIVE SUMMARY

Many bridges in the Unites States are ageing such that they are in need of repair or strengthening. Two key types of damage contributing to the need of bridge repair are girder end cracking and damage caused by vehicular collision. Due to its high strength to weight ratio, corrosion resistance, and increasingly competitive cost, one popular material that can be used for bridge girder repair is fiber reinforced polymer (FRP) composite. The purpose of this research, therefore, is to develop methods and design guidelines for repair and retrofit of bridge girders suffering from: (1) shear strength deficiencies related to end cracking or (2) flexural strength deficiencies related to vehicular collision, specifically by means of FRP composite materials.

This final report contains the results of laboratory testing on scaled test specimens representing bridge girders. Two reinforced concrete (RC) and two prestressed concrete (PC) specimens were prepared and tested. The specimens were subjected to initial damage loading in order to create damage similar to that caused by end cracking and vehicular collision. Additionally, one RC specimen and one PC specimen were repaired with a FRP system consisting of external post-tensioned carbon fiber reinforced polymer (CFRP) rods. After repair, the specimens were loaded to failure

Test results demonstrate that the specimens were successfully repaired such that the repaired specimens had ultimate capacities greater than those of the control specimens. The increase in ultimate capacity was 26.6% and 20.0% for the RC and PC specimens, respectively. It was observed that the repaired specimens failed from rupture of the external CFRP tendons. However, after CFRP failure the specimens exhibited residual strength such that catastrophic beam failure did not occur. The research also demonstrated that a strut-and-tie model is an appropriate design method for the shear controlled RC specimen repaired with the FRP system. Additionally, it was concluded that beam theory is an appropriate design method for the ultimate capacity of the flexure controlled PC specimen repaired with the FRP system as long as the stress in the external CFRP tendons at ultimate can be accurately estimated.

THIS PAGE INTENTIONALLY LEFT BLANK

1.0 INTRODUCTION

1.1 Background Information

Many bridges in the Unites States are ageing such that they are in need of repair or strengthening. If these aging structures do not undergo retrofit procedures, they must be replaced, a procedure much more costly than that of repair. As such, in-situ repair of bridges is more cost effective than replacing the entire structure. One increasingly popular method of retrofit is that of using fiber reinforced polymer (FRP) composite materials. Additionally, the use of FRP is becoming increasingly attractive as the price of FRP decreases. The purpose of this research, therefore, was to develop methods and design guidelines for repair and retrofit of girders using FRP composite materials.

1.2 Project Scope

The scope of this project was focused upon the development of design guidelines that use FRP composite materials for the repair or retrofit of two types of bridge girder damage. The first type of girder damage considered in this research was end girder damage that could result in corrosion of prestressing tendons and mild steel reinforcement and subsequent loss of shear strength. The second type of damage considered in this research is girder damage resulting from impact with vehicles passing underneath the bridge and possible ensuing loss of flexural strength. Illustrative examples of girder end damage and impact damage of prestressed girders can be seen in Figure 1 and Figure 2, respectively.

To develop the abovementioned design guidelines, four scaled test specimens were made. Two of the specimens were designed and tested to simulate girder end cracking resulting in a loss of shear strength, and the other two specimens were designed and tested to simulate flexural damage caused by vehicle impact. Details regarding the design and construction of the laboratory specimens will be discussed in Chapter 2 of this report.

Figure 1 – Girder end damage - 200 East Bridge at I-80

Figure 2 – Girder damage caused by vehicular impact - I-80 bridge in Wanship, UT

1.3 Report Outline

This research project was designed to be carried out in the following sequence:

(a) Preparation and loading of laboratory specimens to simulate the two types of aforementioned damage;

(b) Laboratory testing of the two control specimens and the two FRP repaired specimens to failure.

This final report begins with an explanation of the research methods used, including test specimen design, specimen fabrication and the experimental design. Next, the report will present the methods used for collecting data during laboratory testing of the specimens as well as the loading protocols used on the specimens to inflict initial damage and to fail the control and FRP repaired specimens. An analysis of the results and collected data will also be introduced. Additionally, details of the FRP composite system and how it was applied to the damaged beams will be provided.

THIS PAGE INTENTIONALLY LEFT BLANK

2.0 RESEARCH METHODS

2.1 Overview

The sections in this chapter provide the design and fabrication details of the four scaled concrete beam specimens used in this research. Additionally, the methods used during testing in order to develop girder end cracking and vehicle collision damage are presented in this chapter. Details of the FRP repair system and testing of the specimens to failure are also included.

2.2 Specimen Fabrication

Four scaled beam specimens were designed and fabricated for testing in this project. The size of specimens was determined largely by the geometries of the U of U Structural Testing Laboratory. Two of the beams were reinforced concrete beams, and the other two were prestressed beams. The reinforced concrete (RC) beams were constructed at the University of Utah Structures Laboratory and measure 10 in. wide x 24 in. tall x 9 ft. long. An RC beam was chosen for this geometry due to the difficult nature of prestressing short beams. Both reinforced concrete specimens had similar reinforcement configurations except for differing shear stirrup spacing. The two stirrup spacings used were 8 inches (specimen B8) and 12 inches (specimen B12) on center. The 8 inch spacing was used to represent a correct design, and the 12 inch spacing was used to simulate either an inadequate design or corrosion of properly designed shear reinforcement. Reinforcement details and locations for specimen B8 can be seen in Figure 3.

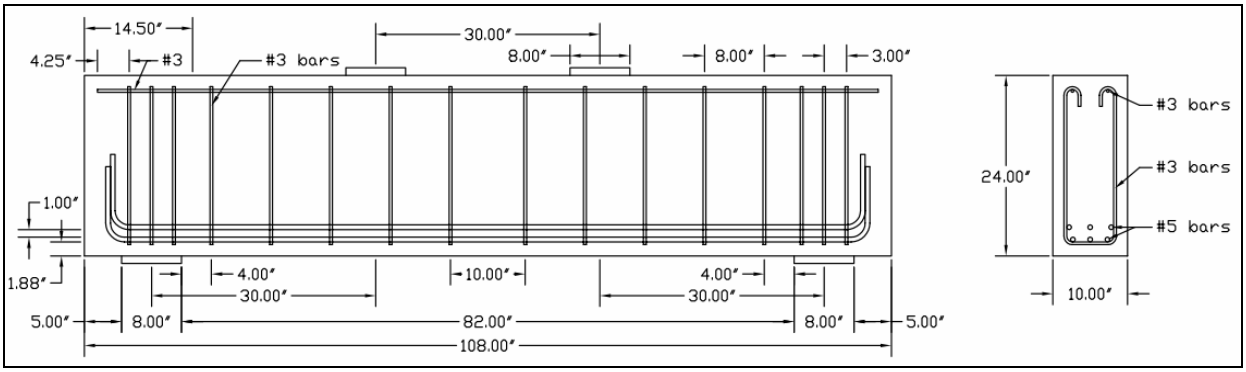

Figure 3 – Reinforcement layout for specimen B8

The two prestressed concrete (PC) girders (specimens P1 and P2) were manufactured by Hanson Eagle Precast at their casting facility and then transported to the University of Utah Structural Testing Laboratory. The precast girders measure 12 in. wide x 20 in. tall x 15 ft. long. Each prestressed beam has three ½ inch 7-wire low-relaxation steel prestressing strands with an ultimate strength of 270 ksi. Additionally, the prestressed beams have #3 stirrups placed at 12 inches on center. Figure 4 shows the reinforcement location for the prestressed beams, and

Table 1 provides a summary of the specimen geometric and reinforcement properties.

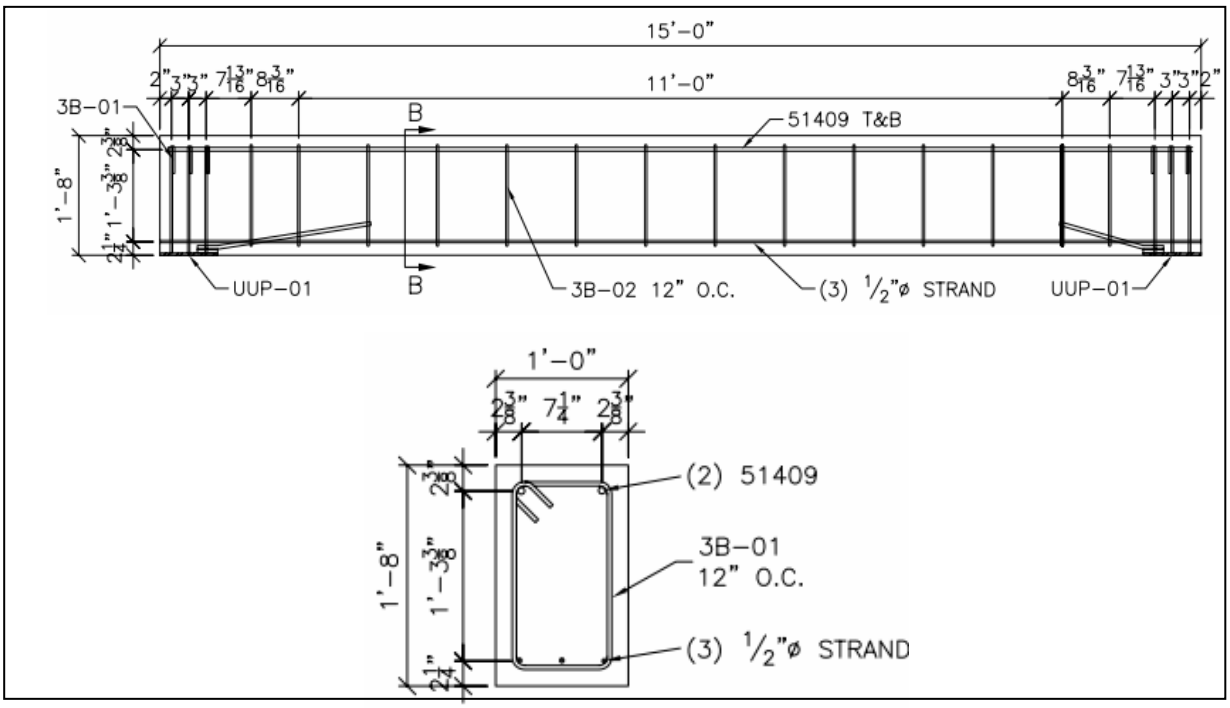

Figure 4 – Reinforcement layout for specimens P1 and P2

Table 1 – Summary of specimen geometric and reinforcement properties

Specimen	Type	Width	Height	Length	Shear Reinforcement	Flexure Reinforcement
B12	RC	10 in.	24 in.	9 ft.	#3 stirrups at 12 in. o.c.	6 - #5 bars
B8	RC	10 in.	24 in.	9 ft.	#3 stirrups at 8 in. o.c.	6 - #5 bars
P1	PC	12 in.	20 in.	15 ft.	#3 stirrups at 12 in. o.c.	3 - ½ in. 7 wire tendons
P2	PC	12 in.	20 in.	15 ft.	#3 stirrups at 12 in. o.c.	3 - ½ in. 7 wire tendons

RC = reinforced concrete
PC = prestressed concrete
o.c. = on center

2.3 Experimental Design

All of the beams were tested in the University of Utah Structural Testing Laboratory. To achieve the simulation of field observed girder end damage and vehicle impact damage, the beams were subjected to a four-point loading system. A 500 kip actuator was used to apply a two point load to the top of the specimens. The distance between the point loads provided by a steel spreader beam was 2 ft-6 in. Additionally, the RC specimens were tested with an unbraced length of 7 ft-6 in., and the PC beams were tested with an unbraced length of 13 ft-8 in. This configuration produced a shear span to depth ratio (a/d ratio) of 1.25 and 3.35 for the reinforced concrete and prestressed beams, respectively. Therefore, the RC beams were designed and loaded to simulate girder end cracking associated with a potential decrease in shear capacity, and the PC beams were designed and loaded to simulate a potential decrease in flexural capacity due to vehicular collision. A diagram of the test setup can be seen in Figure 5.

2.4 Testing Methods and Loading Protocol

Load testing was carried out in two steps - initial damage loading and to failure loading. The initial damage loading was used to introduce girder end cracking damage into the RC specimens and vehicle collision damage into the PC specimens. Next, specimens B8 and P1 were

repaired with external post-tensioned carbon fiber reinforced polymer (CFRP) rods. Finally, the two control specimens and two FRP repaired specimens were loaded to failure. The following sections detail the initial damage loading, the FRP repair, and the loading to failure.

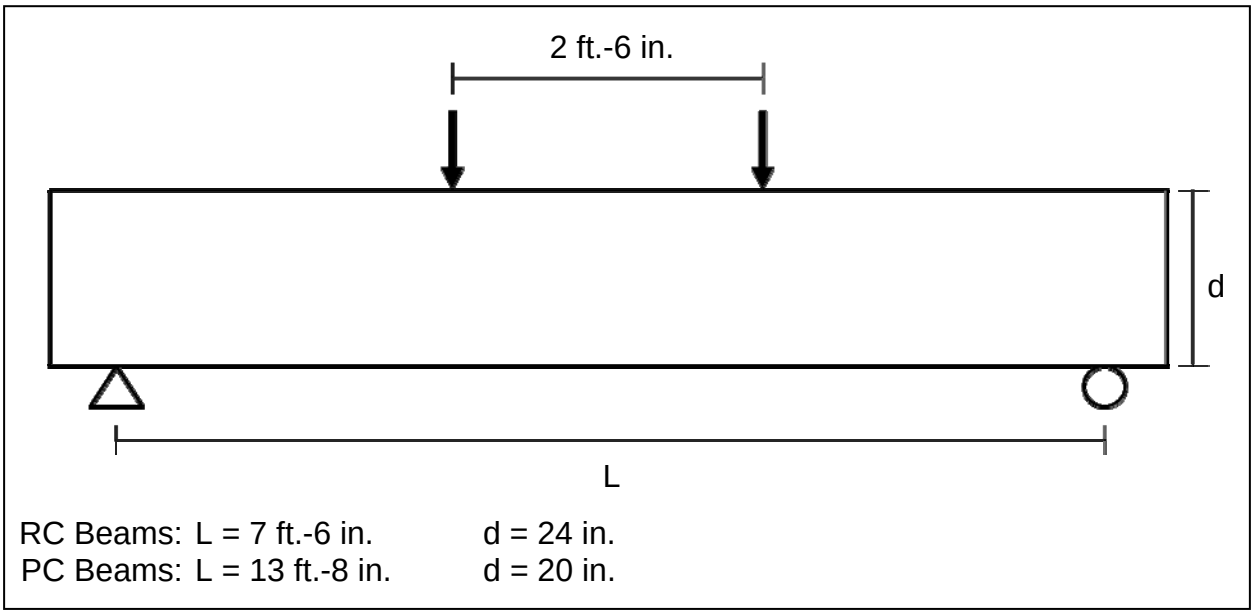

Figure 5 – Test setup

2.4.1 Initial Damage Loading

During the initial damage loading, the test specimens were cyclically loaded to induce cracking and simulate damage seen on full scale girders. The loading was displacement controlled to avoid catastrophic failure and subsequent loss of the specimens. Displacement cycles were carried out in increments of 0.0625 in., with each successive cycle increasing by 0.0625 in. In addition, the rate of displacement was held constant at 0.0625 in./min. throughout the duration of the test. All specimens were subjected to the same loading protocol, with termination of the loading dependent upon visible cracking, deflected shape data, and force versus actuator displacement data. Testing procedures were paused after each cycle to aid in crack inspection, marking, and documentation. An example of the loading protocol used during the initial damage loading is shown in Figure 6.

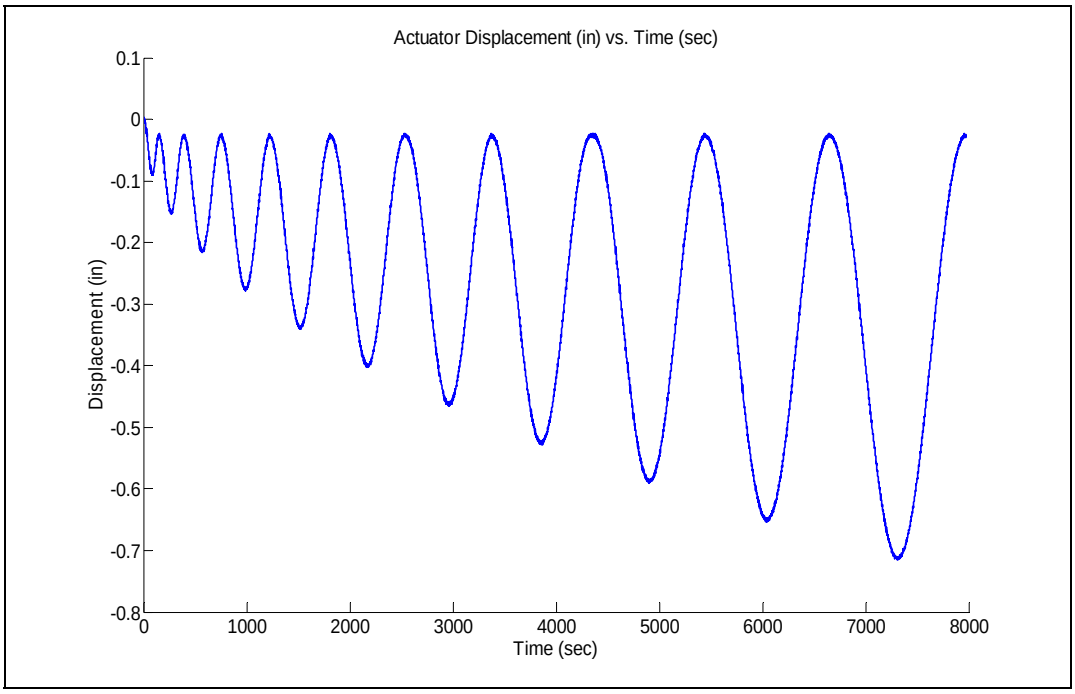

Figure 6 – Loading protocol for specimen B8

In addition to being subject to cracking loads, further damage was inflicted upon specimen P1 to simulate damage from vehicle collision. First, concrete cover was removed to expose an outer 7-wire steel prestressing strand within the constant moment region. Next, three of the seven wires in the strand were cut, leaving specimen P1 with two intact 7-wire strands and one 4-wire strand (three wires were cut). This cut simulated partial severing of the exterior tendon on impact of an exterior girder or corrosion of an exterior tendon due to loss of concrete cover and subsequent exposure to the elements. Figure 7 shows the cut wires.

Figure 7 – Damaged outer steel tendon in specimen P1

2.4.2 FRP Repair

After simulating girder end cracking in the RC specimens and vehicle collision damage in the PC specimens, specimens B8 and P1 were repaired with CFRP composites. The repair consisted of external post-tensioned CFRP rods. The CFRP rods are manufactured by Sika Inc. and have the following properties as provided by the manufacturer: rod diameter = 3/8 in., tensile strength = 27.5 kip, tensile modulus = 22,500 ksi, and elongation at break = 1.1%. Specimen P1 was repaired with a single level of tendons consisting of two rods, one on each side of the beam along the beam length at a depth of 15 in. Specimen B8 was repaired with two levels of tendons consisting of four rods, two on each side of the beam along the beam length at a depth of 11 in. and 19 in.

The CFRP rods were post-tensioned to a strain of approximately 0.485%. This strain produced a post-tensioning force in each rod of about 12 kip. Post-tensioning was accomplished through the use of clamp anchors to grip the rods and a mechanical stressing device to introduce the post-tensioning force. An example of a two tendon layer stressing mechanism can be seen in Figure 8 and Figure 9.

2.4.3 Loading To Failure

After repairing specimens B8 and P1 with external post-tensioned CFRP rods, the specimens were loaded to failure. Additionally, specimens B12 and P2 were loaded to failure as control specimens. The loading to failure was monotonic and conducted at a rate of 0.0625 in./min. Termination of the loading was dependant on failure of the concrete as measured by a 20% decrease in load or failure of the external post-tensioning, whichever came first.

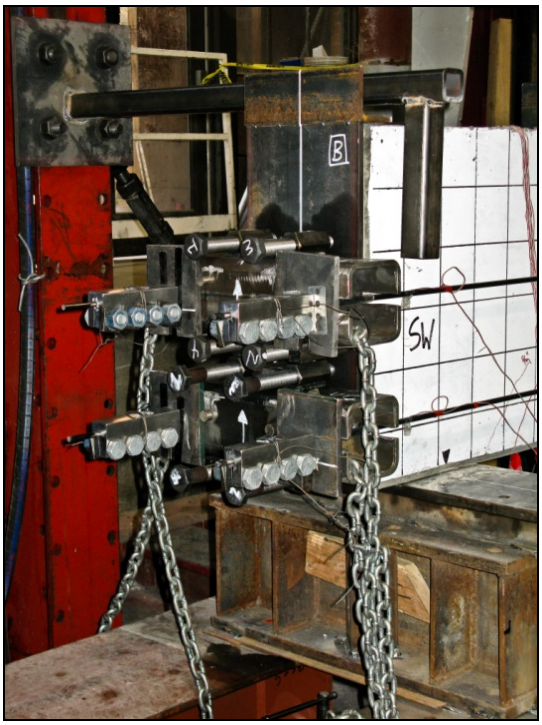

Figure 8 – End view of two level stressing system

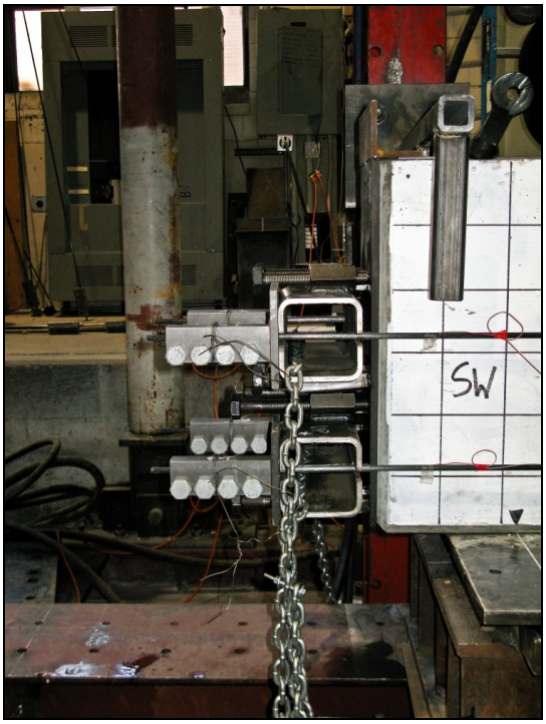

Figure 9 – Side view of two level stressing system

THIS PAGE INTENTIONALLY LEFT BLANK

3.0 DATA COLLECTION

3.1 Overview

The sections in this chapter provide information regarding the method of data collection employed during the research, the type of instruments used, as well as instrumentation locations.

3.2 Data collection Methods

All data from instrumentation was collected by an electronic data acquisition system. The system collected two data points per second. Instrumentation consisted of strain gauges and linear variable differential transformers (LVDTs). All strain gauge readings were measured in units of microstrain, and all LVDT readings were measured in inches.

3.3 Instrumentation Locations

The RC specimens were instrumented with three LVDTs at the bottom of the beam during testing in order to measure the deflected shape under loading. The LVDT locations for RC specimens B12 and B8 were similar and can be seen in Figure 10. Additionally, when specimens B12 and B8 were loaded to failure, concrete strain gauges placed on the top of the beams measured the compressive strain in the concrete. In addition, strain gages were placed on the CFRP rods at midspan to measure the strain in the rods on specimen B8. Similar to the RC beams, during the testing of the PC specimens to failure, concrete strain gauges were placed on the top of the beams to measure the compressive strain in the concrete. In addition, three LVDTs were placed at the bottom of the PC beams during testing to collect deflected shape data. The LVDT locations for PC specimens P1 and P2 were similar and can be seen in Figure 11. Strain gages were placed on the CFRP rods at midspan to measure the strain in the rods on specimen P1. It is also of note that a 500 kip load cell was used to collect force data during all testing procedures. Displacement data for the actuator loading the specimens was also collected.

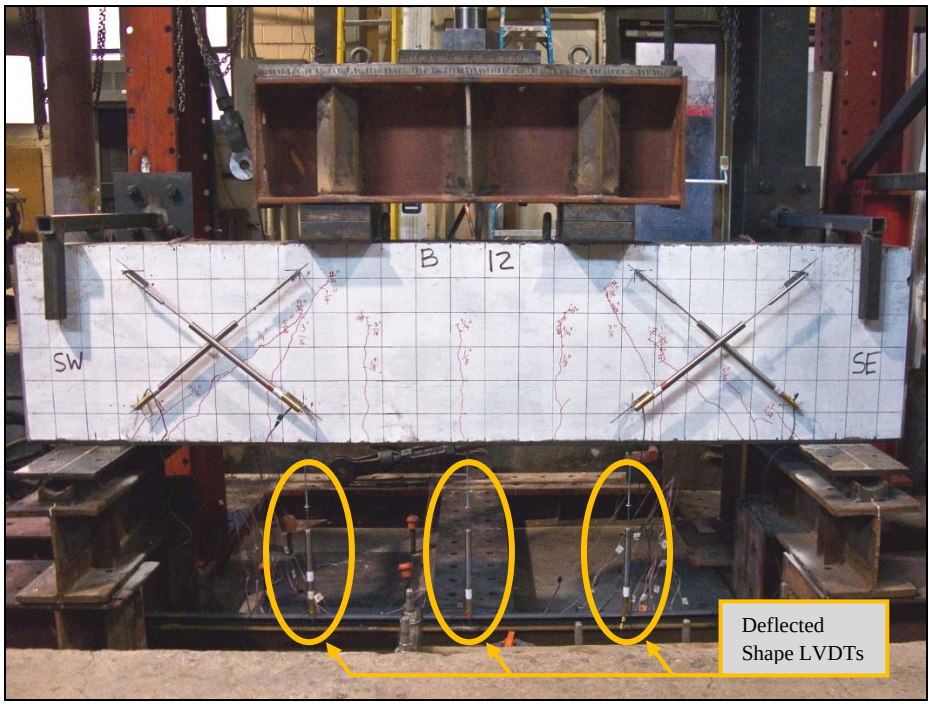

Figure 10 – Specimen B12 LVDT locations

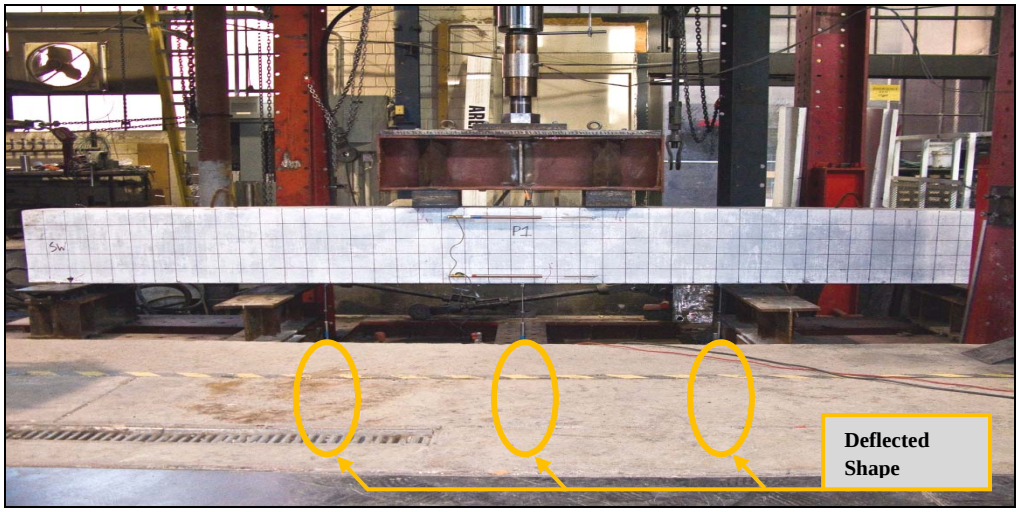

Figure 11 – Specimen P1 LVDT locations

4.0 DATA ANALYSIS

4.1 Overview

The following sections present an analysis and explanation of the collected data and observed cracking and damage of the specimens under loading. Additionally, the properties of the materials used in specimen construction are also presented.

4.2 Material Properties

All steel reinforcing bars used in the fabrication of both the RC and PC specimens had a supplier specified nominal tensile strength of 60 ksi. According to the precast beam manufacturer, the prestressing tendons were low relaxation ½ in. diameter 7-wire strands with a nominal ultimate strength of 270 ksi. Concrete cylinder tests performed at 7 days after casting of the steam cured prestressed beams produced a concrete strength of 7.0 ksi. At the time of specimen testing, the concrete used in the PC beams had a strength of 10.0 ksi. In addition, the strength of the concrete used in the construction of the reinforced concrete specimens at 28 days and at the time of specimen testing was found to be 8.6 ksi and 9.3 ksi, respectively.

4.3 RC Specimen Data Analysis

Several observations can be made from the loading to failure of specimens B12 and B8. During testing, specimen B12 (control) failed from concrete compressive failure between the loading points on top of the beam, and specimen B8 (repaired) failed at later stages from concrete compressive failure between the loading points on top of the beam after rupture of the lower and upper level external CFRP rods. Plots of force versus the midspan deflection during the initial damage loading and the loading to failure for specimens B12 (control) and B8 (repaired) can be seen in Figure 12 and Figure 13. In addition, photos of failed specimens B12 and B8 can be seen in Figure 14 and Figure 15, respectively. It is also of note that the ultimate load for specimens B12 and B8 was 301 kip and 381 kip, respectively. This corresponds to an

increase of approximately 26.6% in ultimate capacity from the use of external post-tensioned CFRP rods.

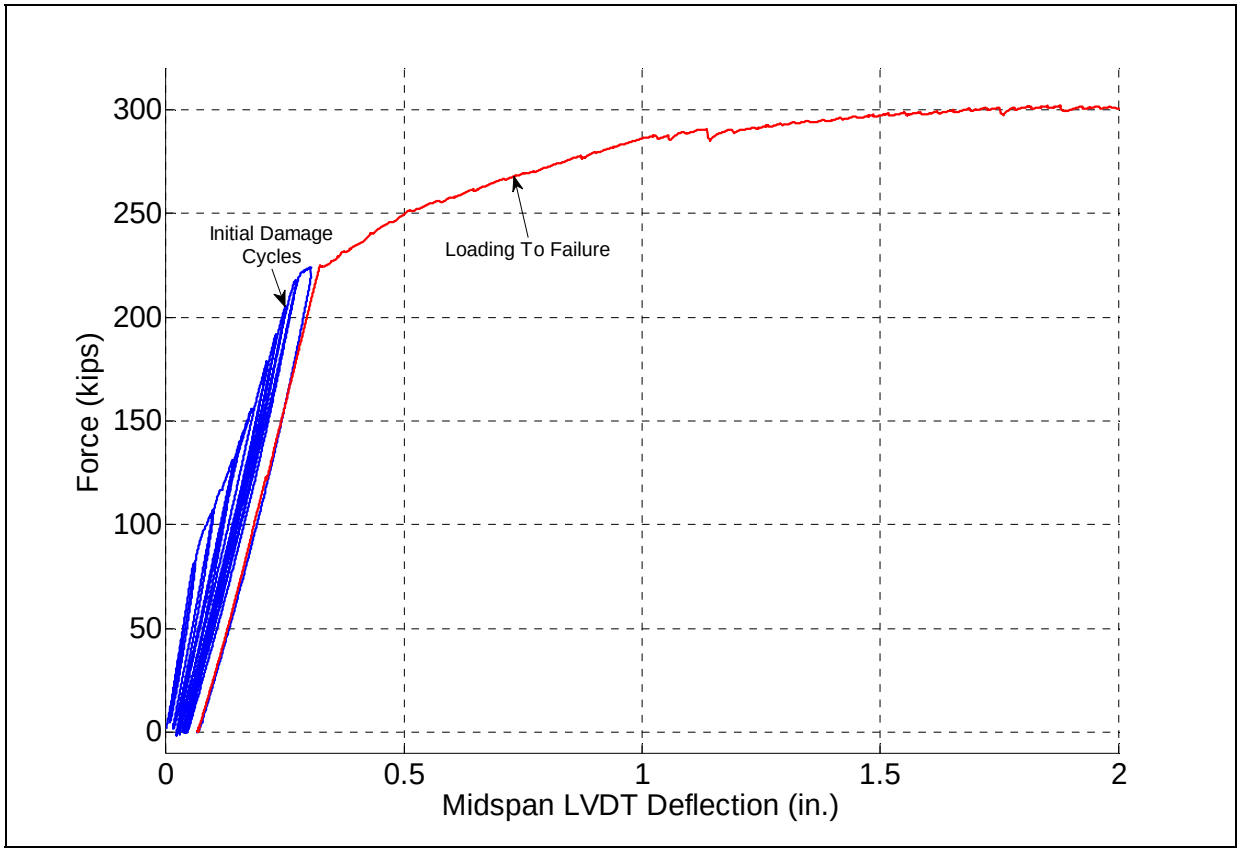

Figure 12 – Force vs. midspan deflection plot for specimen B12 (control)

In addition, the stiffness during loading to failure of specimen B8 (repaired) was found to be 990.9 kip/in., compared to the stiffness of specimen B12 (control) which was 874.0 kip/in. This increase in stiffness can be seen in the linear portion of Figure 16. The stiffness of the RC specimens during the initial damage phase can be found in the interim report related to this research. With respect to deflections, the failure of the bottom layer CFRP rods on specimen B8 occurred at deflections much greater than L/800, the maximum allowable deflection for vehicular loads on concrete construction (AASHTO 2009). Therefore, although the failure of the lower CFRP rods was brittle, the failure occurred at a deflection much greater than service deflections. It can also be seen from Figure 16 that after failure of the upper and lower CFRP rods, specimen B8 exhibited a residual strength of approximately 317 kip. This is evidence that

complete catastrophic failure of the beam did not occur even though brittle failure of the CFRP rods did occur.

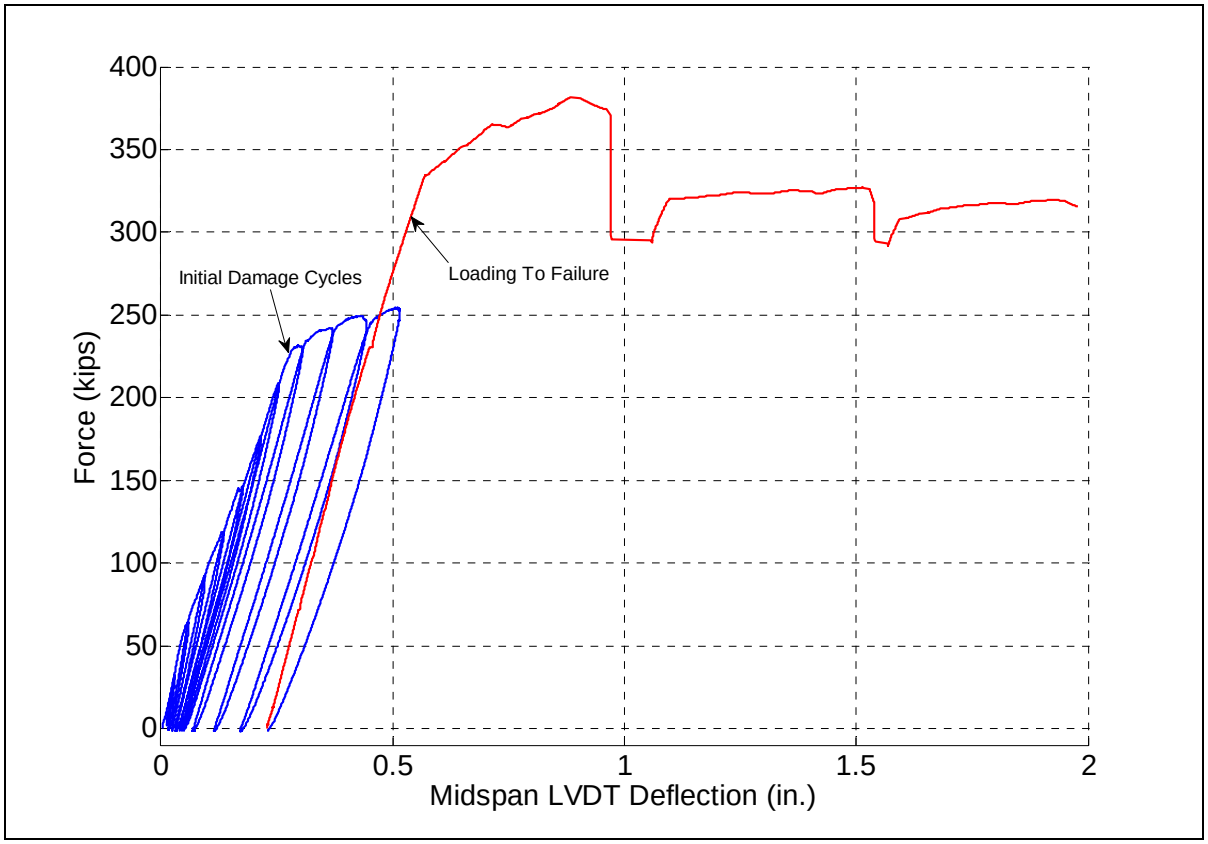

Figure 13 – Force vs. midspan deflection plot for specimen B8 (repaired)

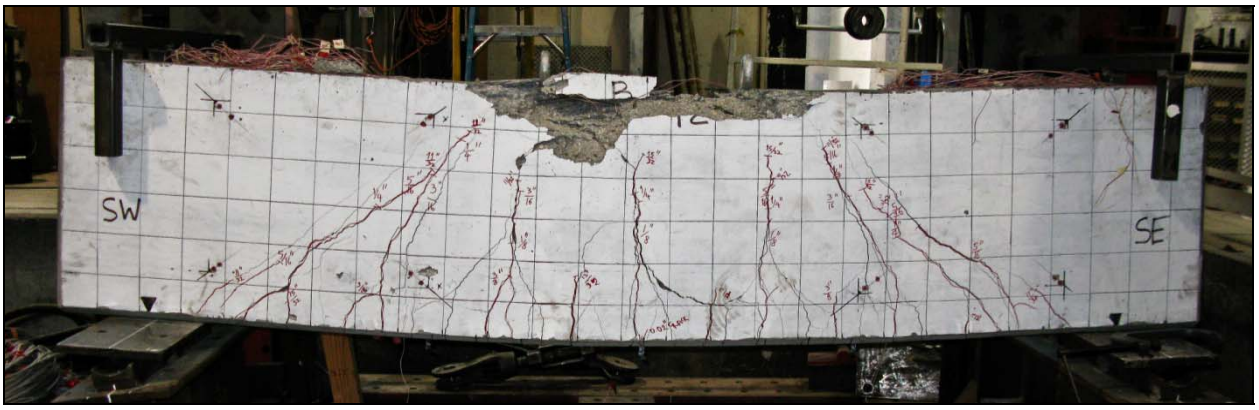

Figure 14 – Specimen B12 (control) after concrete failure

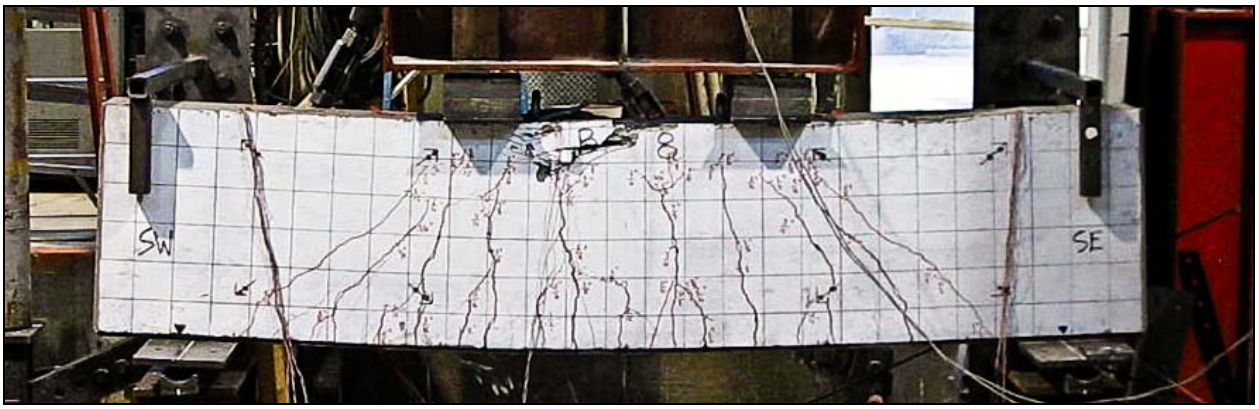

Figure 15 – Specimen B8 (repaired) after CFRP rod rupture and concrete failure

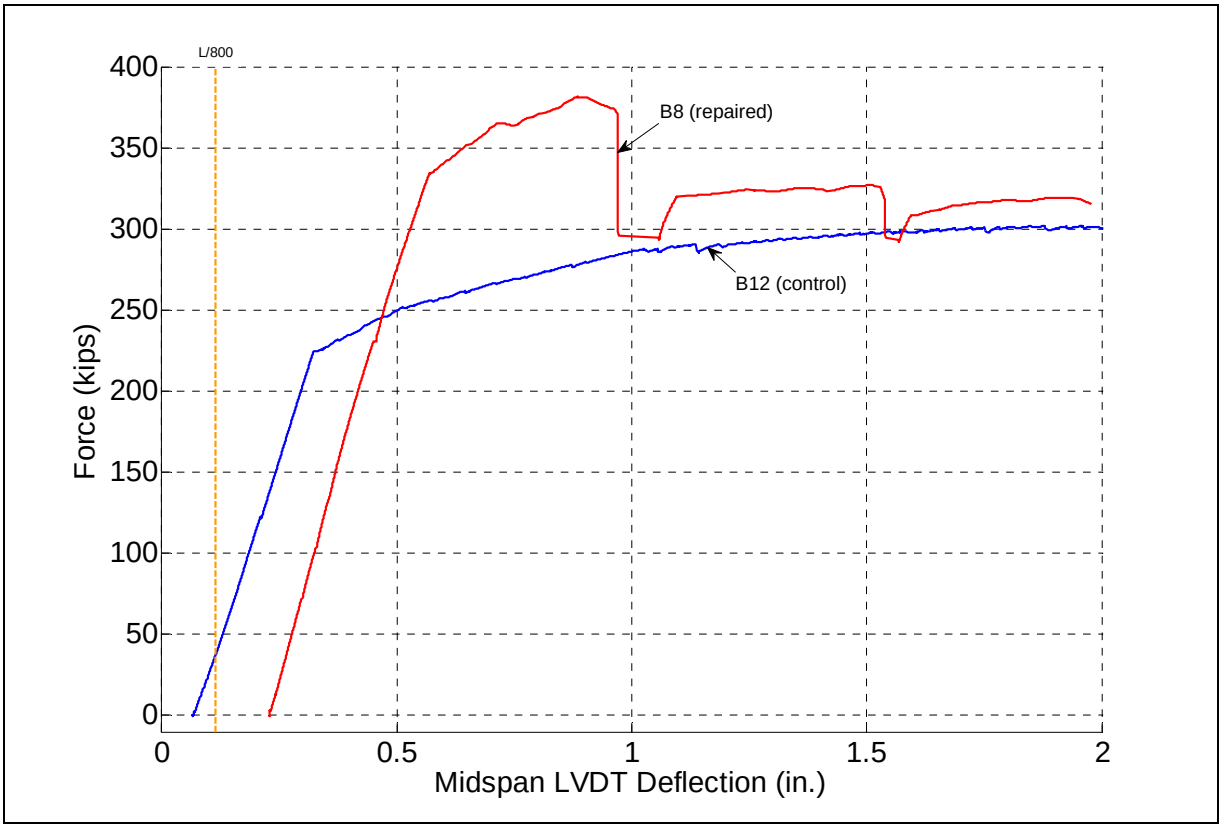

Figure 16 – Force vs. midspan deflection plot for reinforced concrete specimens B12 (control) and B8 (repaired) loaded to failure

An increase in the strain in the CFRP rods in specimen B8 was observed during the testing of the specimen to failure. The initial strain in the rods from the post-tensioning application was 0.485%. At the failure of the lower level external CFRP tendons, the local strain in the lower CFRP rods was approximately 0.903%, and the local strain in the upper CFRP rods was approximately 0.664%. Since the ultimate strain of the rods is 1.1%, there can only be one explanation for rupture of the rods at lower strains – stress concentrations at a point other than where the strain gages were located at midspan.

4.4 PC Specimen Data Analysis

During the testing of the PC specimens, specimen P1 (repaired) failed from rupture of the external CFRP rods and eventual concrete compressive failure, and specimen P2 (control) failed from concrete compressive failure between the loading points on the top of the beam. Photos of specimen P1 (repaired) after rupture of the CFRP rods and specimen P2 (control) after concrete compressive failure can be seen in Figure 17 and Figure 18, respectively.

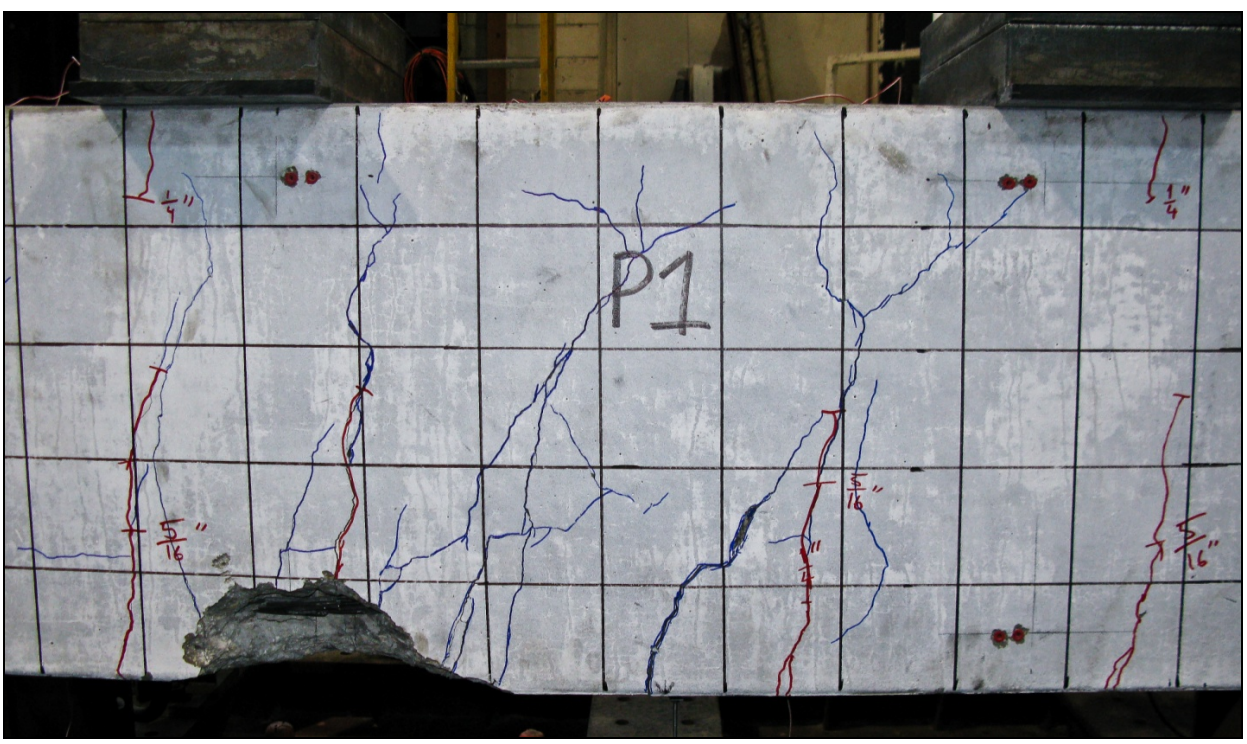

Figure 17 – Specimen P1 (repaired) after CFRP rod rupture

Figure 18 – Specimen P2 (control) after concrete compressive failure

The ultimate load for specimens P1 and P2 was 112 kip and 104 kip, respectively. This corresponds to an increase of approximately 7.7% in ultimate capacity from the use of external post-tensioned CFRP rods. However, it should be remembered that specimen P1 (repaired) had two intact 7-wire strands and one 4-wire strand (three wires were cut), whereas specimen P2 (control) had three intact 7-wire strands. Therefore, application of the theoretical capacity of specimen P1 (repaired) based on the cut wires produces an increase in ultimate capacity of 20.0% from the use of external CFRP rods.

The stiffness during loading to failure of specimen P1 (repaired) and P2 (control) were found to be 400.8 kip/in. and 383.4 kip/in., respectively. This similarity in stiffness can be seen in Figure 19. The stiffness of the PC specimens during the initial damage phase can be found in the interim report related to this research. Additionally, the failure of the CFRP rods on specimen P1 occurred at deflections much greater than L/800, the maximum allowable deflection for vehicular loads on concrete construction (AASHTO 2009). Therefore, although the failure of the CFRP rods was brittle, the failure occurred at a deflection much greater than service deflections. It can also be seen that after failure of the CFRP tendon, specimen P1 (repaired) exhibited a residual strength of approximately 97 kip. This is evidence that complete catastrophic failure of the beam did not occur even though brittle failure of the lower tendons did occur. It can be concluded from Figure 19 that the residual strength in specimen P1 (repaired) after failure of the

CFRP tendons suggests that at large deflections specimen P1 (repaired) would perform similarly to specimen P2 (control) and fail due to concrete compressive failure between the loading points on the top of the beam. However, the capacity of P1 (repaired) would be less than that of specimen P2 (control) due to the cut made to the internal steel tendon of specimen P1 (repaired) during the initial damage loading.

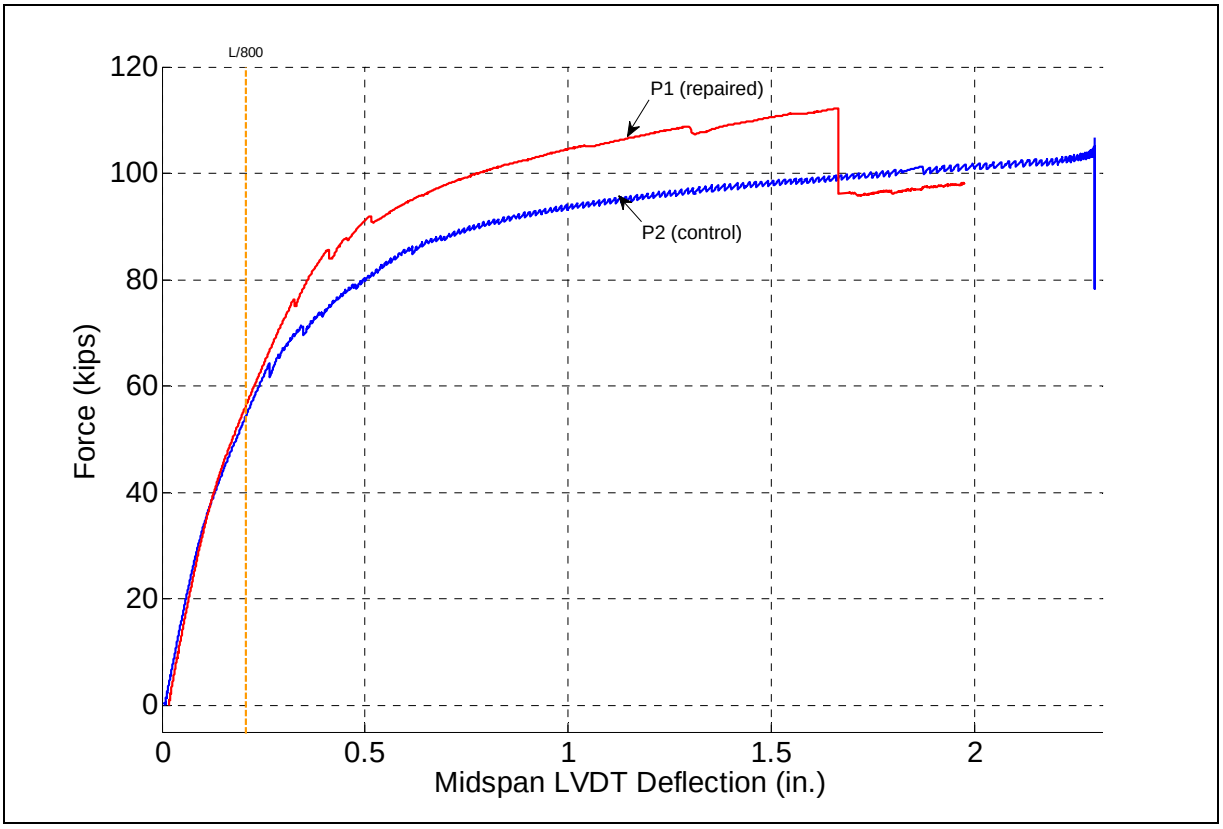

Figure 19 – Force vs. midspan deflection plot for prestressed concrete specimens P2 (control) and P1 (repaired) loaded to failure

An increase in the strain in the CFRP rods in specimen P1 was observed during the testing of the specimen to failure. The initial strain in the rods from the post-tensioning application was 0.485%. At failure of the external CFRP tendons, the strain in the CFRP rods was approximately 0.750%. Since the ultimate strain of the rods is 1.1%, there can only be one explanation for rupture of the rods at lower strains – stress concentrations at a point other than where the strain gages were located at midspan. Additionally, the internal steel prestressing tendons elongated approximately 0.625 in. during testing to failure. This elongation can be seen in Figure 20 and compared visually to Figure 7.

Figure 20 – Elongation in damaged outer steel tendon in specimen P1 (repaired)

4.5 Design Equations

The application of external post-tensioned CFRP tendons in this research is an innovative procedure. As such, it is essential to develop design equations for the prediction of the capacity of the repaired beam specimens. The following sections discuss design equations for the RC specimens and the PC specimens, respectively.

4.5.1 RC Specimen Design Equations

The RC specimen deep beam geometry was selected for its susceptibility to shear controlled failure. This shear controlled failure allowed for the development of damage in the specimens similar to girder end cracking present on full scale bridge girders. Shear controlled failure is common in deep beams like the RC specimens. In practice, it is common for deep beam design to be performed based on a strut-and-tie model. In this research, a strut-and-tie model was used to predict the capacity of specimens B12 (control) and B8 (repaired). Specimen B12 was modeled with a simple strut-and-tie model and can be seen in Figure 21. This model provides a predicted capacity of 176 kip corresponding to a factor of safety of 1.7 based on the actual peak load. Calculations for this model can be found in Appendix A.

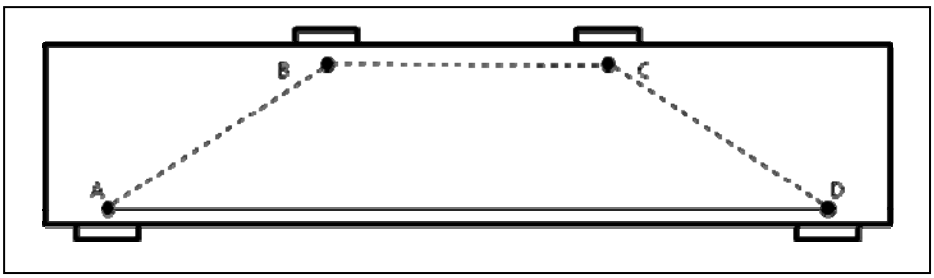

Figure 21 – B12 (control) strut-and-tie model

Specimen B8 was also modeled with a strut-and-tie model. The model used for specimen B8 can be seen in Figure 22. This model provides a predicted capacity of 215 kip which corresponds to a factor of safety of 1.8 based on the actual peak load. The calculations for this model can be found in Appendix B.

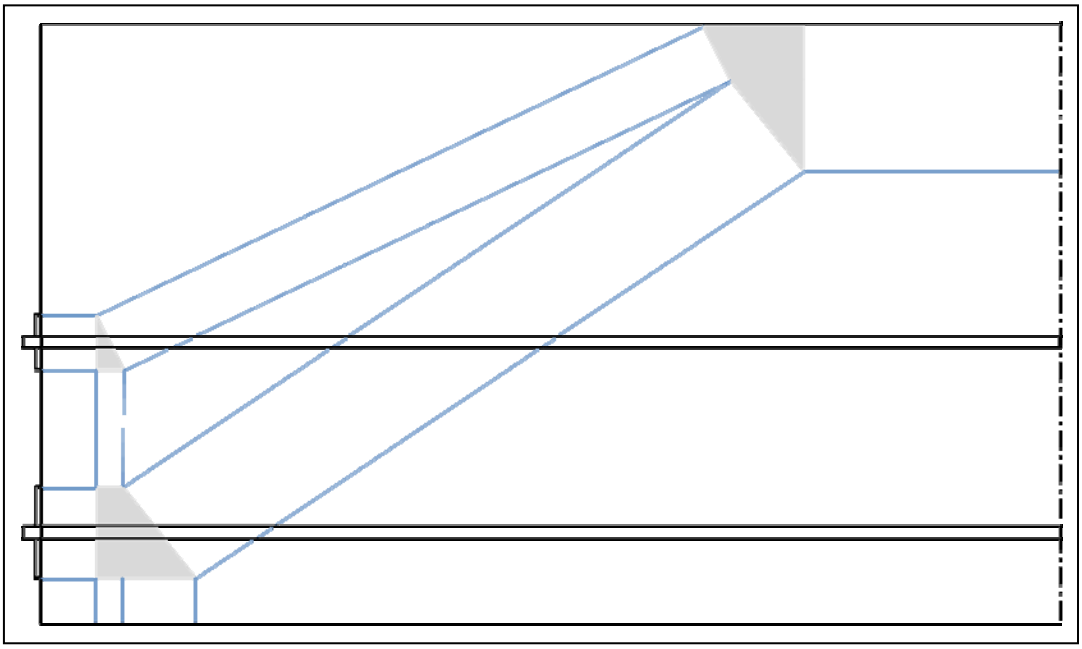

Figure 22 – B8 (repaired) strut-and-tie model

The factors of safety for specimens B12 and B8 are very similar. This similarity in factor of safety suggests that strut-and-tie models provide an acceptable design method for traditional shear controlled reinforced concrete beams as well as shear controlled reinforced concrete beams

repaired with external post-tensioned CFRP rods. A summary of predicted loads, actual loads, and factors of safety for the RC specimens is given in Table 2.

Table 2 – RC specimen peak loads and factors of safety

Specimen	Predicted Peak Load	Actual Peak Load	Factor of Safety
B12 (control)	176 kip	301 kip	1.7
B8 (repaired)	215 kip	381 kip	1.8

4.5.2 PC Specimen Design Equations

The PC specimens were designed with internal high strength low relaxation steel prestressing tendons for their similarity to conventional prestressed bridge girders. In practice, prestressed beams are designed based on conventional beam theory. Conventional beam theory was used to predict peak load for specimen P2 (control). The predicted peak load was 74 kip. Comparing this predicted peak load to the actual peak load produces a factor of safety of 1.4.

While conventional beam theory works well for internal tendons, it is difficult to predict the stress in external tendons at ultimate. Research conducted by Naaman et al. (2002) suggests that the stress at ultimate in external tendons can be found using the following equation.

$$f_{ps} = f_{pe} + \Omega_u E_{ps} \varepsilon_c \left(\frac{d_p}{c} - 1 \right)$$

Where:

f_{ps} is the stress in the external tendons at ultimate
f_{pe} is the prestressing stress in the external tendons
Ω_u is the stress reduction factor
E_{ps} is the modulus of elasticity of the external tendons
ε_c is the failure strain of concrete in compression
d_p is the depth to the external tendons, and
c is the depth of the neutral axis

The application of this equation to determine the stress in the external CFRP tendons at ultimate and conventional beam theory yields a predicted peak load for specimen P1 (repaired) of 84 kip. Comparing to the actual peak load produces a factor of safety of 1.3. The similarity in factors of safety for specimens P1 and P2 demonstrates that use of the abovementioned equation is valid for design purposes. Calculations for the predicted peak loads for specimens P1 and P2 can be found in Appendix C. Additionally, summarizes predicted loads, actual loads, and factors of safety for the PC specimens.

Table 3 – PC specimen peak loads and factors of safety

Specimen	Predicted Peak Load	Actual Peak Load	Factor of Safety	# of strands
P1 (repaired)	84 kip	112 kip	1.3	$2\frac{4}{7}$
P2 (control)	74 kip	104 kip	1.4	3

THIS PAGE INTENTIONALLY LEFT BLANK

7.0 CONCLUSIONS

Based upon the acquired data during testing, it was concluded that specimens B8 and P1 were successfully repaired using external post-tensioned CFRP rods. Specimen B8 showed an increase in stiffness and ultimate strength as compared to the RC control specimen, specimen B12. Therefore, in cases where girder end cracking has occurred, it is feasible to repair the girder with external post-tensioned CFRP rods. The research also demonstrated that a strut-and-tie model is an applicable design method for shear controlled beams repaired with external post-tensioned CFRP rods.

Successful repair with external post-tensioned CFRP rods was also observed in the PC specimens. Specimen P1 (repaired) showed an increase in ultimate strength and comparable stiffness compared to the PC control specimen, specimen P2. This increase in ultimate strength occurred even with a partially severed tendon. Additionally, it was found that beam theory provides applicable design equations for flexure controlled concrete beams. However, the stress in the external CFRP rods at ultimate must be calculated.

It is also of note that although the repaired specimens failed as a result of rupture of the external CFRP rods, the rupture occurred at deflections much greater than service deflections. In addition, residual capacity was present after CFRP rod rupture. This is significant in that catastrophic beam failure did not occur even though the CFRP tendons failed.

This report has summarized the research and has provided the following information:

- Details of specimen fabrication
- Details of damage inflicted on specimens
- Details of the FRP system used for repair
- Experimental results from testing specimens to failure
- Design methods and equations for predicting ultimate capacity of FRP repaired specimens.

THIS PAGE INTENTIONALLY LEFT BLANK

APPENDIX A: B12 (CONTROL) CAPACITY CALCULATIONS

Tie:

$num_bars := 6$ $\quad space_between_tie_rows := 1.0in$

$d_{tie_bar} := 0.625in$ $\quad A_{s_prov} := num_bars \cdot 0.31 \cdot in^2 = 1.86in^2$

Geometry Variables:

$h := 24in$ $\quad b := 10in$ $\quad l := 90in$ $\quad l_n := 82in$

$cc := 1.5in$ Minimum is 1.5" per ACI 7.7.1

$d := h - cc - 0.5 \cdot space_between_tie_rows - d_{tie_bar} = 21.375in$

$shear_span := 30in$

$d_c := cc + d_{tie_bar} + 0.5 \cdot space_between_tie_rows = 2.625in$

Concrete:

$f'_c := 9300psi$

Bars:

$f_y := 63000psi$

Find the depth to nodes:

$$a := \frac{A_{s_prov} \cdot f_y}{0.85 \cdot f'_c \cdot b} = 1.482 \cdot in$$

$depth_to_top_node_1 := 0.5 \cdot a = 0.741 \cdot in$

$depth_to_top_node_2 := 0.05 \cdot h = 1.2 \cdot in$

$depth_to_top_node := depth_to_top_node_1 = 0.741 \cdot in$

Check ?:

$vert_proj_of_strut := h - depth_to_top_node - d_c = 20.634in$

$horiz_proj_of_strut := 30in$

$$\theta := atan\left(\frac{h - 2 \cdot depth_to_top_node}{30in}\right) = 36.891 \cdot deg$$

$$\theta_check := \begin{cases} \text{"}\theta \text{ is OK"} & \text{if } \theta \geq 25deg \\ \text{"}\theta \text{ is NOT OK"} & \text{otherwise} \end{cases}$$

$\theta_check = \text{"}\theta \text{ is OK"}$

Find the Force in the Tie:

$F_{tie_AD} := A_{s_prov} \cdot f_y = 117.18kip$

Find the Forces in the Struts and P:

$$F_{strut_AB} := \frac{F_{tie_AD}}{\cos(\theta)} = 146.516kip$$

$F_{strut_BC} := F_{strut_AB} \cdot \cos(\theta) = 117.18\,kip$

$P := F_{strut_AB} \cdot \sin(\theta) = 87.954\,kip$ $\qquad$ $P = 87.954\,kip$

Horizontal Reinforcement:

Assume $s_{horiz_reinf} := 8in$

$A_{vh_min} := 0.0015\,b \cdot s_{horiz_reinf} = 0.12in^2$

$A_{vh} := 2 \cdot 0.11in^2$ $\qquad$ $d_{b_horizontal} := 0.375in$

$$check_A_{vh} := \begin{cases} \text{"Avh is OK"} & \text{if } A_{vh} > A_{vh_min} \\ \text{"Avh is NOT OK"} & \text{otherwise} \end{cases}$$

$check_A_{vh} = \text{"Avh is OK"}$

Vertical Reinforcement:

$A_v := 2 \cdot 0.11in^2$ $\qquad$ $d_{stirrup} := 0.375in$

$force_per_stirrup := A_v \cdot f_y = 13.86\,kip$

$$num_of_vertical_stirrups := \frac{P}{force_per_stirrup} = 6.346$$

$$s_{vert_reinf} := \frac{l}{num_of_vertical_stirrups} = 14.182in$$

Say $s_{vert_reinf} := 8in$

Check A.3.3.1:

$\alpha_2 := \theta = 36.891\,deg$ $\qquad$ $\alpha_1 := 90deg - \alpha_2 = 53.109\,deg$

$$sum := \frac{A_{vh}}{b \cdot s_{horiz_reinf}} + \frac{A_v}{b \cdot s_{vert_reinf}} = 0.00550$$

$$check_grid_reinf := \begin{cases} \text{"Grid reinf. is OK"} & \text{if } sum > 0.003 \\ \text{"Grid reinf. is NOT OK"} & \text{otherwise} \end{cases}$$

$check_grid_reinf = \text{"Grid reinf. is OK"}$

Calculate Effective Concrete Strengths:

$$\beta_s := \begin{pmatrix} 1.000 \\ 0.750 \\ 0.600 \\ 0.400 \\ 0.600 \end{pmatrix} \begin{array}{l} \text{Uniform cross section} \\ \text{Bottle - reinforced} \\ \text{Bottle - unreinforced} \\ \text{Tension members} \\ \text{All other cases} \end{array}$$

$f_{ce_struts} := 0.85 \cdot \beta_{s_{1,1}} \cdot f'_c = 7.905\,ksi$

$$\beta_n := \begin{pmatrix} 1.00 \\ 0.80 \\ 0.60 \end{pmatrix} \begin{matrix} \text{CCC} \\ \text{CCT} \\ \text{CTT} \end{matrix}$$

$$f_{ce_A} := 0.85 \cdot \beta_{n_{2,1}} \cdot f'_c = 6.324\,\text{ksi}$$

$$f_{ce_D} := f_{ce_A} = 6.324\,\text{ksi}$$

$$f_{ce_B} := 0.85 \cdot \beta_{n_{1,1}} \cdot f'_c = 7.905\,\text{ksi}$$

$$f_{ce_C} := f_{ce_B} = 7.905\,\text{ksi}$$

Determine Available Node and Strut Widths:

$l_b := 8\text{in}$ Say $w_{prov_strut_BC} := 5\text{in}$ since $a = 1.482\text{in}$ Say $w_{t_AD} := 2 \cdot d_c = 5.25\text{in}$

Node A:

$$w_{prov_A_incline} := w_{t_AD} \cdot \cos(\theta) + l_b \cdot \sin(\theta) = 9.001\text{in}$$

$$w_{prov_A_horizontal} := l_b = 8\,\text{in}$$

$$w_{prov_A_vertical} := w_{t_AD} = 5.25\text{in}$$

Node B:

$$w_{prov_B_incline} := w_{prov_strut_BC} \cdot \cos(\theta) + l_b \cdot \sin(\theta) = 8.801\text{in}$$

$$w_{prov_B_horizontal} := l_b = 8\,\text{in}$$

$$w_{prov_B_vertical} := w_{prov_strut_BC} = 5\,\text{in}$$

Determine Required Node and Strut Widths:

$$w_{req_strut_AB} := \frac{F_{strut_AB}}{0.75 \cdot f_{ce_struts} \cdot b} = 2.471\text{in}$$

$$w_{req_strut_BC} := \frac{F_{strut_BC}}{0.75 \cdot f_{ce_struts} \cdot b} = 1.976\text{in}$$

$$w_{req_A_incline} := \frac{F_{strut_AB}}{0.75 \cdot f_{ce_A} \cdot b} = 3.089\text{in}$$

$$w_{req_A_horizontal} := \frac{P}{0.75 \cdot f_{ce_A} \cdot b} = 1.854\text{in}$$

$$w_{req_A_vertical} := \frac{F_{tie_AD}}{0.75 \cdot f_{ce_A} \cdot b} = 2.471in$$

$$w_{req_B_incline} := \frac{F_{strut_AB}}{0.75 \cdot f_{ce_B} \cdot b} = 2.471in$$

$$w_{req_B_horizontal} := \frac{P}{0.75 \cdot f_{ce_B} \cdot b} = 1.484in$$

$$w_{req_B_vertical} := \frac{F_{strut_BC}}{0.75 \cdot f_{ce_B} \cdot b} = 1.976in$$

Check Strength of Struts, Nodes, and Bearing Capacity:

$$check_Strut_AB_1 := \begin{cases} \text{"Strut AB is OK at Node A"} & \text{if } w_{prov_A_incline} \geq w_{req_strut_AB} \\ \text{"Strut AB is NOT OK at Node A"} & \text{otherwise} \end{cases}$$

$$check_Strut_AB_2 := \begin{cases} \text{"Strut AB is OK at Node B"} & \text{if } w_{prov_B_incline} \geq w_{req_strut_AB} \\ \text{"Strut AB is NOT OK at Node B"} & \text{otherwise} \end{cases}$$

$$check_Strut_BC_1 := \begin{cases} \text{"Strut BC is OK at Node A"} & \text{if } w_{prov_A_incline} \geq w_{req_strut_BC} \\ \text{"Strut BC is NOT OK at Node A"} & \text{otherwise} \end{cases}$$

$$check_Strut_BC_2 := \begin{cases} \text{"Strut BC is OK at Node B"} & \text{if } w_{prov_B_incline} \geq w_{req_strut_BC} \\ \text{"Strut BC is NOT OK at Node B"} & \text{otherwise} \end{cases}$$

$$check_Node_A_1 := \begin{cases} \text{"Incline face is OK"} & \text{if } w_{prov_A_incline} \geq w_{req_A_incline} \\ \text{"Incline face is NOT OK"} & \text{otherwise} \end{cases}$$

$$check_Node_A_2 := \begin{cases} \text{"Horizontal face is OK"} & \text{if } w_{prov_A_horizontal} \geq w_{req_A_horizontal} \\ \text{"Horizontal face is NOT OK"} & \text{otherwise} \end{cases}$$

$$check_Node_A_3 := \begin{cases} \text{"Vertical face is OK"} & \text{if } w_{prov_A_vertical} \geq w_{req_A_vertical} \\ \text{"Vertical face is NOT OK"} & \text{otherwise} \end{cases}$$

$$check_Node_B_1 := \begin{cases} \text{"Incline face is OK"} & \text{if } w_{prov_B_incline} \geq w_{req_B_incline} \\ \text{"Incline face is NOT OK"} & \text{otherwise} \end{cases}$$

$$check_Node_B_2 := \begin{cases} \text{"Horizontal face is OK"} & \text{if } w_{prov_B_horizontal} \geq w_{req_B_horizontal} \\ \text{"Horizontal face is NOT OK"} & \text{otherwise} \end{cases}$$

$$check_Node_B_3 := \begin{cases} \text{"Vertical face is OK"} & \text{if } w_{prov_B_vertical} \geq w_{req_B_vertical} \\ \text{"Vertical face is NOT OK"} & \text{otherwise} \end{cases}$$

$$\sigma_A := \frac{P}{0.75 \cdot b \cdot l_b} = 1466psi \qquad \sigma_B := \frac{P}{0.75 \cdot b \cdot l_b} = 1466psi$$

$$check_bearing_A := \begin{cases} \text{"Bearing at A is OK"} & \text{if } \sigma_A \le 0.75 f_{ce_A} \\ \text{"Bearing at A is NOT OK"} & \text{otherwise} \end{cases}$$

$$check_bearing_B := \begin{cases} \text{"Bearing at B is OK"} & \text{if } \sigma_B \le 0.75 f_{ce_B} \\ \text{"Bearing at B is NOT OK"} & \text{otherwise} \end{cases}$$

$$check_Strut_AB = \begin{pmatrix} \text{"Strut AB is OK at Node A"} \\ \text{"Strut AB is OK at Node B"} \end{pmatrix}$$

$$check_Strut_BC = \begin{pmatrix} \text{"Strut BC is OK at Node A"} \\ \text{"Strut BC is OK at Node B"} \end{pmatrix}$$

$$check_Node_A = \begin{pmatrix} \text{"Incline face is OK"} \\ \text{"Horizontal face is OK"} \\ \text{"Vertical face is OK"} \end{pmatrix}$$

$$check_Node_B = \begin{pmatrix} \text{"Incline face is OK"} \\ \text{"Horizontal face is OK"} \\ \text{"Vertical face is OK"} \end{pmatrix}$$

$$check_bearing_A = \text{"Bearing at A is OK"}$$

$$check_bearing_B = \text{"Bearing at B is OK"}$$

Check Tie:

$$A_{s_prov} = 1.86 in^2$$

$$A_{s_req} := \frac{F_{tie_AD}}{f_y} = 1.86 in^2$$

$$check_Tie_AD := \begin{cases} \text{"Tie is OK"} & \text{if } \left| A_{s_prov} - A_{s_req} \right| \le 0.00001 in^2 \\ \text{"Tie is NOT OK"} & \text{otherwise} \end{cases} \qquad check_Tie_AD = \text{"Tie is OK"}$$

If all checks are OK then P is governed by the A_s in the tie and $P = 88 \cdot kip$

$$2 \cdot P = 176 \cdot kip$$

Factor of Safety:

$$P_{actual} := 301 kip$$

$$FS_{B12} := \frac{P_{actual}}{2 \cdot P} = 1.7$$

THIS PAGE INTENTIONALLY LEFT BLANK

APPENDIX B: B8 (REPAIRED) CAPACITY CALCULATIONS

Concrete Properties:

$f'_c := 9300psi$ $\quad E_c := 57000\sqrt{f'_c \cdot psi^{-1}} \cdot psi = 5497 \cdot ksi$

Reinforcement Properties:

$f_y := 63000psi$

Assume 6#5 bars: $A_s := 6 \cdot 0.31in^2$ and $d_b := 0.625 \cdot in$

Assume #3 stirrups: $A_v := 2 \cdot 0.11 \cdot in^2$ and $d_{b_v} := 0.375in$

CFRP Rod Properties:

$E_{rod} := 22.5 \cdot 10^6 psi$ $\quad A_{rod} := 0.11in^2$ $\quad \varepsilon_{u_rod} := 1.1\%$

Specimen Geometry:

Beam height: $h := 24in$

Beam width: $b := 10in$

Shear span: $shear_span := 30in$

Length of bearing pad: $l_b := 8in$

Depth to top CFRP tendons: $d_2 := 11in$

Depth to bottom CFRP tendons: $d_1 := 19in$

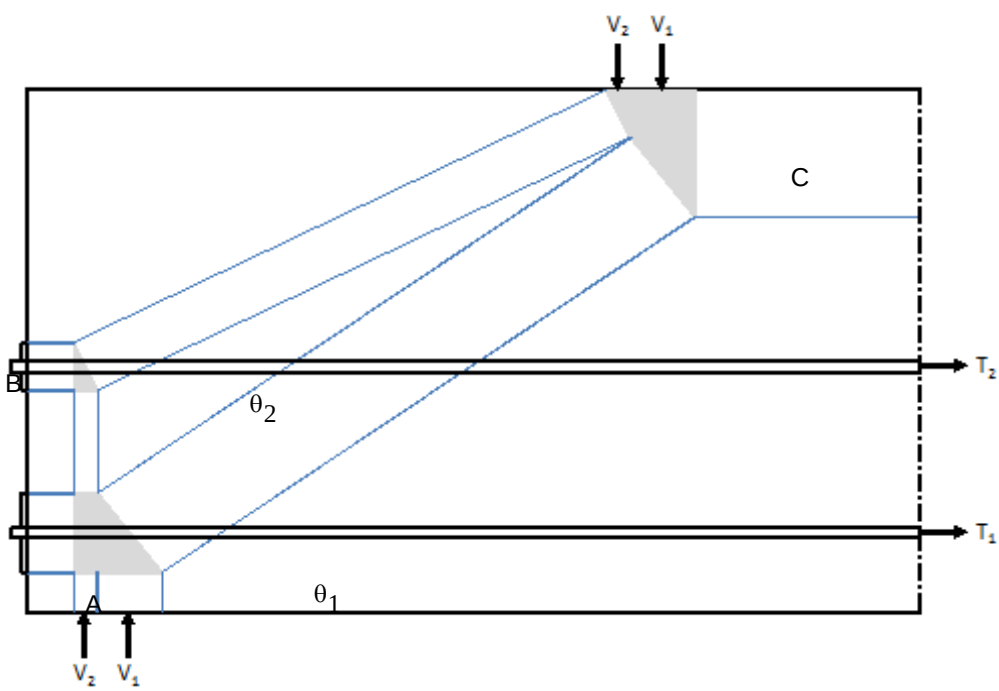

Capacity Calculations:

$$a := \frac{A_s \cdot f_y}{0.85 \cdot f'_c \cdot b} = 1.482 \cdot in$$

Assumption: The height of node B is: $w_{prov_B_vert} := a$

$$\theta_2 := atan\left(\frac{d_2 - \frac{1}{3} \cdot w_{prov_B_vert}}{shear_span}\right) = 19.3 \cdot deg$$

Assumption: The height of node A is: $w_{prov_A_vert} := 6in$

$$\theta_1 := atan\left(\frac{d_1 - w_{prov_B_vert} - \frac{1}{3} w_{prov_A_vert}}{shear_span}\right) = 27.35 \cdot deg$$

Assumption: The maximum tendon strains are: $\varepsilon_{max_1} := 82\% \cdot \varepsilon_{u_rod}$ and $\varepsilon_{max_2} := 82\% \cdot \varepsilon_{u_rod}$

$$T_1 := E_{rod} \cdot \varepsilon_{max_1} \cdot A_{rod} = 22.325 \cdot kip$$

$$T_2 := E_{rod} \cdot \varepsilon_{max_2} \cdot A_{rod} = 22.325 \cdot kip$$

$$T_{steel} := A_s \cdot f_y = 117.18 \cdot kip$$

$$V_2 := \tan(\theta_2) \cdot T_2 = 7.818 \cdot kip$$

$$V_{1_tendon} := \tan(\theta_1) \cdot T_1 = 11.547 \cdot kip$$

$$V_{1_steel} := \tan(37deg) \cdot T_{steel} = 88.301 \cdot kip$$

$$V_{total} := V_{1_tendon} + V_{1_steel} + V_2 \qquad V_{total} = 107.7 \cdot kip$$

$$2 \cdot V_{total} = 215 \cdot kip$$

Factor of Safety:

$$P_{actual} := 381 kip$$

$$FS_{B8} := \frac{P_{actual}}{2 \cdot V_{total}} = 1.8$$

APPENDIX C: P1 (REPAIRED) AND P2 (CONTROL) CAPACITY CALCULATIONS

$f'_c := 10000psi$ $\varepsilon_{cu} := 0.003$

Mild Steel Properties:

$f_y := 63000psi$

$A_s := 2 \cdot 0.31in^2$

$A_{s_top} := 2 \cdot 0.31in^2$

Prestressing Steel Properties:

$A_{tendon} := 0.153in^2$ $f_{pu} := 270000psi$ $num_steel_tendons := 3$

CFRP Properties:

$E_{FRP} := 22.5 \cdot 10^6 psi$ $A_{FRP} := 2 \cdot 0.11in^2$ $\varepsilon_{u_FRP} := 1.1\%$

THIS PAGE INTENTIONALLY LEFT BLANK

$\varepsilon_{pe_FRP} := 0.485\%$

Specimen Geometry:

$h := 20in$ $b := 12in$ $L := 15ft - 12in - 4in$

$d_p := h - 2.25in = 17.75 \cdot in$

$d := 15in$

$d_{top} := \left(2 + \frac{3}{8}\right) \cdot in$

$d_{FRP} := 15in$

$P_{P1_actual} := 112kip$

$P_{P2_actual} := 104kip$

Capacity Calculations:

$f_{py} := 0.90 f_{pu} = 243000\,psi$

Stress Relieved = $0.85 f_{pu}$
Low-relaxation = $0.90 f_{pu}$

$$\beta_1 := \max\left[0.85 - \frac{0.05\cdot\left(f'_c - 4000psi\right)}{1000psi}, 0.65\right] = 0.65$$

Assumption: $f_{ps} := f_{py}$

Specimen P2 (control):

$A_{ps} := num_steel_tendons \cdot A_{tendon} = 0.459\,in^2$

$$a := \frac{A_{ps}\cdot f_{ps} + A_s\cdot f_y + A_{s_top}\cdot f_y}{0.85 f'_c\cdot b} = 1.859\,in$$

$$M_n := A_{ps}\cdot f_{ps}\cdot\left(d_p - \frac{a}{2}\right) + A_s\cdot f_y\cdot\left(d - \frac{a}{2}\right) + A_{s_top}\cdot f_y\cdot\left(d_{top} - \frac{a}{2}\right) = 206.844\,kip\cdot ft$$

$$P_{P2} := \frac{M_n}{0.5L - 15in}$$

$P_{P2} = 37\cdot kip$

$2\cdot P_{P2} = 74\cdot kip$

$$FS_{P2} := \frac{P_{P2_actual}}{2\cdot P_{P2}} = 1.4$$

Specimen P1 (repaired):

$f_{pe_FRP} := E_{FRP}\cdot\varepsilon_{pe_FRP} = 1.091\times 10^5\cdot psi$

$$A_{ps} := \frac{7\cdot 3 - 3}{7\cdot 3}\cdot num_steel_tendons \cdot A_{tendon} = 0.393\,in^2$$

Calculate capacity of beam with cut wires and no FRP repair...

$$a := \frac{A_{ps}\cdot f_{ps} + A_s\cdot f_y + A_{s_top}\cdot f_y}{0.85 f'_c\cdot b} = 1.703\,in$$

$$M_n := A_{ps}\cdot f_{ps}\cdot\left(d_p - \frac{a}{2}\right) + A_s\cdot f_y\cdot\left(d - \frac{a}{2}\right) + A_{s_top}\cdot f_y\cdot\left(d_{top} - \frac{a}{2}\right) = 185.64\,kip\cdot ft$$

$$P_{P1_cut_no_FRP} := \frac{M_n}{0.5L - 15in} \qquad P_{P1_cut_no_FRP} = 33.2 \cdot kip$$

Calculate capacity of beam with cut wires and FRP repair...

Assumption: $f_{u_FRP} := 199985 psi$ <-- Manually change this value until it matches the value below

$$a := \frac{A_{ps} \cdot f_{ps} + A_s \cdot f_y + A_{s_top} \cdot f_y + A_{FRP} \cdot f_{u_FRP}}{0.85 f'_c \cdot b} = 2.135 \cdot in$$

$$c := a \cdot \beta_1 = 1.387 \cdot in$$

$$\Omega_u := \frac{1.5}{\frac{L}{d_{FRP}}} = 0.137$$

$$f_{u_FRP} := f_{pe_FRP} + \Omega_u \cdot E_{FRP} \cdot \varepsilon_{cu} \cdot \left(\frac{d_{FRP}}{c} - 1 \right) = 199985 psi$$

$$M_n := A_{ps} \cdot f_{ps} \cdot \left(d_p - \frac{a}{2} \right) + A_s \cdot f_y \cdot \left(d - \frac{a}{2} \right) + A_{s_top} \cdot f_y \cdot \left(d_{top} - \frac{a}{2} \right) \ldots = 233.601 \cdot kip \cdot ft$$
$$+ A_{FRP} \cdot f_{u_FRP} \cdot \left(d_{FRP} - \frac{a}{2} \right)$$

$$P_{P1} := \frac{M_n}{0.5L - 15in} \qquad P_{P1} = 41.8 \cdot kip$$

$$2 \cdot P_{P1} = 84 \cdot kip$$

$$FS_{P1} := \frac{P_{P1_actual}}{2 \cdot P_{P1}} = 1.3 \qquad \frac{P_{P1_actual} - P_{P2_actual}}{P_{P2_actual}} = 7.7 \cdot \%$$

Estimated values based on FS for no FRP tendons and cut wires...

$$FS_{P1_from_cut} := \frac{P_{P1_actual}}{2 \cdot P_{P1_cut_no_FRP} \cdot FS_{P2}} = 1.2 \qquad \frac{P_{P1_actual} - 2 \cdot P_{P1_cut_no_FRP} \cdot FS_{P2}}{2 \cdot P_{P1_cut_no_FRP} \cdot FS_{P2}} = 20.0 \cdot \%$$

THIS PAGE INTENTIONALLY LEFT BLANK

REFERENCES

American Association of State Highway and Transportation Officials. (2009). *AASHTO LRFD Bridge Design Specifications* (4th Edition ed.).

American Concrete Institute. (2008). Building Code Requirements for Reinforced Concrete (ACI 318-08) and Commentary (ACI 318R-08). Detroit: American Concrete Institute.

Naaman, A., Burns, N., French, C., Gamble, W., & Mattock, A. (2002). Stresses in Unbonded Prestressing Tendons at Ultimate: Recommendation. *ACI Structural Journal , 99* (4), 518-529.

Pantelides, C., Reaveley, L., & Burningham, C. (2008). *Repair of Concrete Girder Ends and Girder Collision Repair with CFRP Post-Tensioned Rods: Interim Report.* Salt Lake City: Utah Department of Transportation.

THIS PAGE INTENTIONALLY LEFT BLANK

ACRONYMS

ACI – American Concrete Institute

FRP – Fiber reinforced Polymer

LVDT – Linear variable differential transformer

PC – Prestressed concrete

RC – Reinforced concrete

U of U – University of Utah

UDOT – Utah Department of Transportation